Electrically-controlled rapid femtosecond pulse duration switching and continuous picosecond pulse duration tuning in an ultrafast Cr^{4+}:forsterite laser.

C. Crombie,[1] D. A. Walsh,[1] W. Lu,[2] S. Zhang,[3] Z. Zhang,[3] K. Kennedy,[3] S. Calvez,[2,4] W. Sibbett,[1] and C.T.A. Brown[1,*]

[1]*SUPA, School of Physics and Astronomy, University of St Andrews, St Andrews, Fife KY16 9SS, UK*
[2]*Institute of Photonics, University of Strathclyde, Glasgow, UK*
[3]*EPSRC National Centre for III-V Technologies, University of Sheffield, Sheffield, UK*
[4]*Currently at LAAS-CNRS, 7 avenue du Colonel Roche, 31077, Toulouse, CDEX 4, France*
[*]*ctab@st-andrews.ac.uk*

Abstract: We demonstrate rapid switching between picosecond and femtosecond operational regimes in a Cr^{4+}:forsterite laser, using an electrically-contacted GaInNAs SESAM with saturable absorption characteristics controlled via the quantum-confined Stark effect. Additionally, continuous picosecond pulse duration tuning by over a factor 3 is reported.

OCIS codes: (320.7160) Ultrafast technology; (140.4050) Mode-locked lasers; (140.3580) Solid-state lasers; (140.7090) Ultrafast lasers; (260.6580) Stark effect; (250.5590) Quantum-well, -wire and -dot devices.

References and links

1. W. Sibbett, A. A. Lagatsky, and C. T. A. Brown, "The development and application of femtosecond laser systems," Opt. Express **20**(7), 6989–7001 (2012).
2. S. Tsuda, W. H. Knox, S. T. Cundiff, W. Y. Jan, and J. E. Cunningham, "Mode-locking ultrafast solid-state lasers with saturable Bragg reflectors," IEEE J. Sel. Top. Quantum Electron. **2**(3), 454–464 (1996).
3. U. Keller, K. J. Weingarten, F. X. Kartner, D. Kopf, B. Braun, I. D. Jung, R. Fluck, C. Honninger, N. Matuschek, and J. Aus der Au, "Semiconductor saturable absorber mirrors (SESAM's) for femtosecond to nanosecond pulse generation in solid-state lasers," IEEE J. Sel. Top. Quantum Electron. **2**(3), 435–453 (1996).
4. V. G. Savitski, D. Burns, and S. Calvez, "Optically-pumped saturable absorber for fast switching between continuous-wave and passively mode-locked regimes of a Nd:YVO(4) laser," Opt. Express **17**(7), 5373–5378 (2009).
5. V. G. Savitski, N. K. Metzger, S. Calvez, D. Burns, W. Sibbett, and C. T. A. Brown, "Optical trapping with "on-demand" two-photon luminescence using Cr:LiSAF laser with optically addressed saturable Bragg reflector," Opt. Express **20**(7), 7066–7070 (2012).
6. B. Stormont, E. U. Rafailov, I. G. Cormack, A. Mooradian, and W. Sibbett, "Extended-cavity surface-emitting diode laser as active mirror controlling modelocked Ti: sapphire laser," Electron. Lett. **40**(12), 732–734 (2004).
7. A. A. Lagatsky, E. U. Rafailov, W. Sibbett, D. A. Livshits, A. E. Zhukov, and V. M. Ustinov, "Quantum-dot-based saturable absorber with p-n junction for mode-locking of solid-state lasers," IEEE Photon. Technol. Lett. **17**(2), 294–296 (2005).
8. S. A. Zolotovskaya, K. G. Wilcox, A. Abdolvand, D. A. Livshits, and E. U. Rafailov, "Electronically controlled pulse duration passively modelocked Cr: forsterite laser," IEEE Photon. Technol. Lett. **21**(16), 1124–1126 (2009).
9. D. A. B. Miller, D. S. Chemla, T. C. Damen, A. C. Gossard, W. Wiegmann, T. H. Wood, and C. A. Burrus, "Band-edge electroabsorption in quantum well structures - the quantum-confined Stark-effect," Phys. Rev. Lett. **53**(22), 2173–2176 (1984).
10. C. T. A. Brown, D. J. Stevenson, X. Tsampoula, C. McDougall, A. A. Lagatsky, W. Sibbett, F. J. Gunn-Moore, and K. Dholakia, "Enhanced operation of femtosecond lasers and applications in cell transfection," J Biophoton. **1**(3), 183–199 (2008).
11. V. Liverini, S. Schon, R. Grange, M. Haiml, S. C. Zeller, and U. Keller, "Low-loss GaInNAs saturable absorber mode locking a 1.3-mu m solid-state laser," Appl. Phys. Lett. **84**(20), 4002–4004 (2004).

#169611 - $15.00 USD Received 30 May 2012; revised 17 Jul 2012; accepted 17 Jul 2012; published 23 Jul 2012

12. A. McWilliam, A. A. Lagatsky, C. G. Leburn, P. Fischer, C. T. A. Brown, G. J. Valentine, A. J. Kemp, S. Calvez, D. Burns, M. D. Dawson, M. Pessa, and W. Sibbett, "Low-loss GaInNAs saturable Bragg reflector for mode-locking of a femtosecond Cr4+: Forsterite-laser," IEEE Photon. Technol. Lett. **17**(11), 2292–2294 (2005).
13. R. Grange, A. Rutz, V. Liverini, M. Haiml, S. Schon, and U. Keller, "Nonlinear absorption edge properties of 1.3-mu m GaInNAs saturable absorbers," Appl. Phys. Lett. **87**(13), 132103 (2005).
14. J. Misiewicz, P. Sitarek, G. Sek, and R. Kudrawiec, "Semiconductor heterostructures and device structures investigated by photoreflectance spectroscopy," Mater. Sci.-Poland **21**, 263–320 (2003).
15. S. L. Chuang, *Physics of Photonic Devices* 1 ed., Wiley Series in Pure and Applied Optics (Wiley,2009).
16. P. Cerný, G. Valentine, D. Burns, and K. McEwan, "Passive stabilization of a passively mode-locked laser by nonlinear absorption in indium phosphide," Opt. Lett. **29**(12), 1387–1389 (2004).
17. F. X. Kärtner and U. Keller, "Stabilization of solitonlike pulses with a slow saturable absorber," Opt. Lett. **20**(1), 16–18 (1995).

1. Introduction

In recent years ultrafast laser technology has found uses in a wide and ever growing range of applications [1]. Initially this success was based largely on Kerr-lens mode-locked (KLM) lasers but the development of semiconductor-based saturable absorber elements brought robust turnkey enhancement to the mode-locked operation [2, 3]. Recently, it has also become desirable to improve the functionality of ultrafast lasers through further adaptability in their temporal performance. Specifically, in this work we show how external electrical control of a semiconductor saturable absorbing mirror (SESAM) can enable pulse-duration tuning over several orders of magnitude.

The work of Savitski *et al.* [4] has shown that optical control of a SESAM through induced localized heating close to the control laser beam focus can be effective in altering the absorption spectrum of a quantum-well saturable absorber. They have also demonstrated the use of such lasers in optical trapping experiments where controlled two-photon responses can be achieved [5]. This work showed that, while acceptable pulse-duration tuning was possible, it required the use of an additional laser with focus parameters that ensured an optimum overlap with the intracavity laser field. A simpler approach is either to influence the optical properties of the SESAM without recourse to a separate laser or to implement slower and therefore less versatile bulk-heating of the device. Earlier studies by Stormont *et al.* [6] Lagatsky *et al.* [7] and Zolotovskaya *et al.* [8] had confirmed that it is possible to bring some electrical external control to a SESAM to alter the output of mode-locked lasers. In their work, Stormont et al. used a quantum well based vertical extended-cavity surface-emitting laser device as a saturable absorber in a Ti:sapphire laser operating around 950 nm. By an appropriate application of reverse bias, they could observe switching between cw operation and pulses for 100's ps duration [6]. By contrast, Lagatsky et al. and Zolotovskaya et al. used electrically contacted quantum dot devices as saturable absorbers and obtained pulse duration tuning from 10 ps to 6.8 ps at 1029 nm [7] and 17.4 ps to 6.4 ps around 1280 nm [8].

By reverse biasing a custom-designed, electrically-contacted SESAM, it is possible to exploit the quantum-confined Stark effect (QCSE) [9] to change the optical absorption properties of a quantum-well saturable absorber. This enables direct electrical control of the pulse duration through the control of the amplitude of the fast saturable change in reflectance, and also enables the saturable absorption to be turned on/off, thereby switching mode-locking on/off, if the shift in absorption wavelength is sufficient. In the work reported here, we not only demonstrate the application of a bespoke GaInAs quantum-well-based SESAM in a Cr^{4+}:forsterite laser for pulse-duration tuning in the picosecond-pulse regime by a factor of 3.2 (1.9 ps to 6.1 ps), but we also show, for the first time to the authors' knowledge, that it is possible to induce a rapid (as short as 20 μs) change in the operational regime from cw to picosecond and from picosecond to femtosecond through direct electrical control of the SESAM alone. Our preliminary assessments also indicate a potential for this technique to facilitate rapid switching between the cw and the femtosecond regimes.

Possible applications for this level of control include implementations in biophotonics where it is desirable to have control of the pulse duration (and hence peak power) whilst

#169611 - $15.00 USD Received 30 May 2012; revised 17 Jul 2012; accepted 17 Jul 2012; published 23 Jul 2012

maintaining a constant average laser power. One example of such a requirement arises in switching between optical tweezing and photo-poration [10] when a single laser is used.

2. SESAM design, fabrication and characterization

To provide device performance comparisons, two SESAM samples were prepared for this evaluation. The first device was uncontacted and similar to existing SESAM designs for use in this spectral region [11]. The second device was electrically-contacted to enable the application of a reverse bias to induce a change in device performance via the quantum-confined Stark effect. Given that in a quantum well, the Stark shift manifests itself as a modulation of the effective band gap, in a quantum-well SESAM this means that it is possible to induce an exploitable bias-induced change in the absorption spectrum. The SESAM absorption performance can thereby be wavelength tuned to facilitate a real-time active control of its function within the laser. Within the present context, changes in primary characteristics of the SESAM ranging from saturable absorption to high reflectivity at a particular wavelength through the application of a suitable electric field are especially relevant.

The PCB-mounted, wire-bonded contacted device used in our assessments is shown in Fig. 1(a). The top surface contacts had an aperture-based matrix so that the intracavity light field could be coupled efficiently into a single element of the device. This design strategy required a careful balance to be achieved between apertures that were sufficiently small to ensure a uniform electric field across the semiconductor, but sufficiently large to accommodate the focal spot of the intracavity beam. Our device was designed with aperture sizes that ranged from 50 µm to 200 µm in diameter, although in practice only the largest of these apertures were wire bonded.

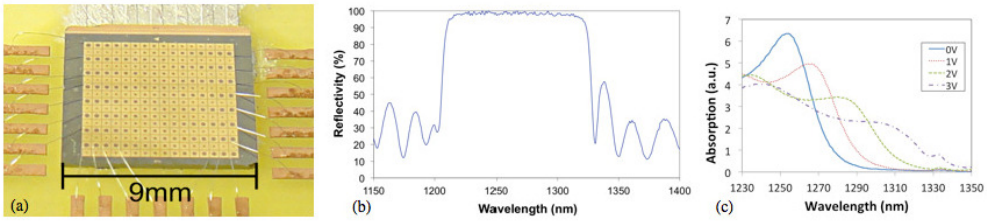

Fig. 1. (a) Photograph of the contacted QCSE SESAM where the inner diameter of the top electrical contacts ranged from 50 µm to 200 µm. (b) Measured linear reflectivity curve for the QCSE device. (c) Field-induced absorption change derived from the photocurrent response of a 200 µm-diameter QCSE SESAM.

The QCSE anti-resonant SESAM epilayer was grown by molecular beam epitaxy on an n-doped (100) GaAs substrate and consists of a n-doped 35.5-repeats of $Al_{0.5}Ga_{0.5}As$(20 nm)/AlAs(89.8 nm)/ $Al_{0.5}Ga_{0.5}As$(20 nm)/GaAs(73.6 nm) distributed Bragg reflector with a center wavelength = 1262 nm, an insulating λ/2-thick GaAs layer in the middle of which is a single 8 nm thick $Ga_{0.62}In_{0.38}N_{0.016}As_{0.984}$ QW and a p-doped λ-thick top GaAs layer. The contacted devices were defined to have a planar InSe/Au n-contact, 50 µm-wide Au/Zn/Au ring p-contacts with inner diameter ranging from 50 µm to 200 µm and Si_3N_4-insulated 460 µm square Ti/Au bonding pads. The linear reflectivity curve for the device is shown in Fig. 1(b). The saturation fluence for the device (inferred from the laser mode-locking threshold) was found to be ~60 µJ/cm^2. Based on previous studies by McWilliam et al. [12] on similar devices, the non-saturable losses for this SESAM were expected to be low (< 1%) and the modulation depth was expected to be ~0.1%.

The absorption properties of the SESAM were characterized by measuring the photocurrent response and Fig. 1(c) shows the change in wavelength-dependent absorption as a function of applied reverse bias. The characteristic behavior expected due the QCSE can be observed clearly where, as the reverse bias is increased, the absorption peak of the quantum

#169611 - $15.00 USD Received 30 May 2012; revised 17 Jul 2012; accepted 17 Jul 2012; published 23 Jul 2012

well red shifts and weakens. As a consequence, these electrically-induced performance modifications allow real-time active control of the SESAM function within a laser, notably from saturable absorption to high reflectivity around 1300 nm. Whilst it is apparent that these measurements are taken at conditions that are some way from the operating conditions within a laser cavity, previous work by Grange et al. [13] on GaInNAs SESAMs has shown that they provide a reasonable guide to the properties of the device when operating in this wavelength region.

To characterize more precisely the dependence of the QW bandgap on the applied reverse field, spectroscopic photo-reflectance measurements [14] were carried out on the contacted sample and the recorded signals together with the identified bandgap positions are shown in Fig. 2(a). The measured shift in bandgap with applied bias, as shown in Fig. 2(b), is in good agreement with the theoretical predictions obtained for an infinitely deep quantum well [15].

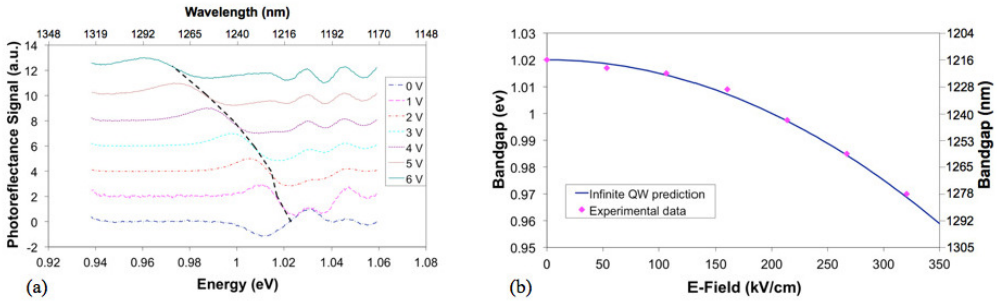

Fig. 2. (a) Photo-reflectance characterization of the response of a 200 μm diameter QCSE SESAM. The curves are vertically offset for enhanced visibility. The dashed line indicates the bandgap energy. (b) Field-induced bandgap change derived from the photo-reflectance response of a 200 μm diameter QCSE SESAM with calculated values. The applied E-field is taken to be the result of the applied voltage across the 187.2 nm thick intrinsic region of the device i.e. we assume negligible voltage drops across the doped regions.

3. Results and discussion

The laser resonator was configured as in Fig. 3(a) for these investigations. It was formed from a z-shaped astigmatically-compensated design containing a 22 mm long Brewster-cut Cr^{4+}:forsterite rod with intracavity fused silica prisms for dispersion compensation. The intracavity beam spot diameter on the SESAM of 80 μm was chosen to be compatible with the 200 μm aperture SESAMs such that losses due to beam-clipping on the edge of the aperture could be minimized. When operated with a high reflectivity (HR) mirror at the SESAM location and with a 2% output coupler, the laser produced an output power of 530 mW at a center wavelength of 1265 nm. When this HR mirror was replaced with the uncontacted SESAM the output power characteristics for the laser are as shown in Fig. 3(b). The laser operated cw until the mode-locking threshold for femtosecond pulse generation that was found to be around 10 mW laser output power with the 2% output coupler. This behavior implied a reasonable performance for this design of SESAM [12] and clearly demonstrated the low non-saturated losses expected for the device. The output pulses were characterized using a Femtochrome FR103MN intensity autocorrelator and the output spectrum was measured using an IST Rees spectrum analyzer. Pulses as short as 285 fs were obtained with a bandwidth of 6 nm centered at 1265 nm and the repetition frequency of the laser was 165 MHz. The corresponding time-bandwidth product of 0.32 indicated a transform-limited performance. It was also possible to obtain shorter pulses from these SESAMs by increasing the pump power (and hence the output power from the laser) when pulse durations as short as 74 fs were obtained. However, when operated in this latter regime, the pulsed output was less stable and was unsuitable for the assessment of switching performance.

#169611 - $15.00 USD Received 30 May 2012; revised 17 Jul 2012; accepted 17 Jul 2012; published 23 Jul 2012

The uncontacted SESAM was then replaced by the contacted device and the intracavity spot on the SESAM was adjusted to be accommodated fully within one of the 200 µm apertures and the output power characteristics of the laser in this configuration are shown by the red symbols and line in Fig. 3(b).. The similarity in the average-power performance for the resonators that incorporated the uncontacted (black line in Fig. 3(b)) and contacted SESAMs, shows that the fabrication process for the apertures and the laser alignment had not added significantly to intracavity losses. In a free-running operation (without an intracavity slit for wavelength control), the preferred lasing center wavelength was 1265nm but, when a slit was used, tuning could be affected from 1215 nm to 1300 nm to enable advantage to be taken of the tuning behavior of the biased SESAM.

To observe switching behavior, the output beam of the laser was tightly focused onto a Si detector. When the laser generated ultrashort pulses a signal was observed on this detector due to the induced two-photon absorption. The nonlinear response of this detector was confirmed and enabled operation in cw, picosecond and femtosecond regimes to be distinguished readily. The results were also confirmed by autocorrelation and radio frequency spectrum analyzer (RFSA) measurements when the laser was operating in steady state.

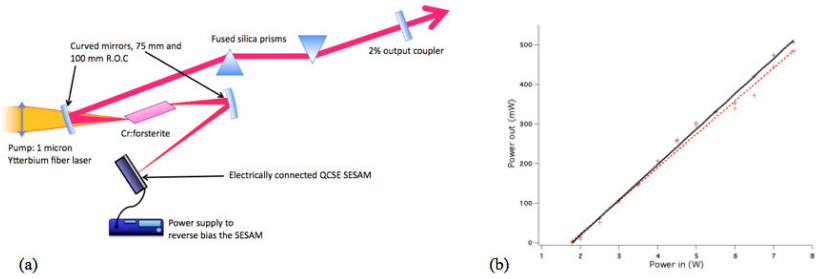

Fig. 3. (a) Schematic of the laser resonator, incorporating a pair of fused silica prisms and a Brewster-cut Cr^{4+}:forsterite crystal. (b) Power characteristics of the laser with contacted (red) and uncontacted (black) SESAMs.

The SESAM was reverse biased at 4 V to obtain regime switching. This induced a change from femtosecond operation at 1257 nm with pulse durations of 285 fs to picosecond operation at 1272 nm with pulse durations of 6.4 ps whilst maintaining a constant average output power of 25 mW. All pulse durations were calculated on the assumption of $sech^2$ pulse intensity profiles and these were near the transform limit. As confirmed by the data of Fig. 4(a), the transient switching time from femtosecond to picosecond operation was around 20 µs and around 200 µs for the switch back. The repeatability of this behavior is demonstrated in Fig. 4(b) for a voltage modulation frequency of 300 Hz. The bias-switching threshold around 2 V was optimum for this particular laser at 4 V and the application of higher reverse bias values caused the laser operation to become unstable.

The laser was then wavelength-tuned to achieve picosecond to cw switching at around 1283 nm. The laser produced output powers of 82 mW when mode locked (with pulse duration of 116 ps) and 77 mW when operating in the continuous wave (cw) un-mode-locked regime. When the SESAM was reverse biased at a voltage of 3 V, successful switching between mode-locked picosecond and cw operation was observed as confirmed by Fig. 5(a). The switching time from cw to ps was found to be ~50 µs with a switch-off time of around 200 µs. With this methodology, it would be desirable to be able to switch directly from cw to mode locking in the femtosecond regime, but although it was possible to access both un-mode-locked and femtosecond-mode-locked operation an increased applied reverse bias in the same spectral region, (see Fig. 5(b)) the operation was not stable and some transitioning between temporal operation regimes can be observed during periods of continuously applied reverse bias. This was attributed to the laser operating at the edge of its performance

#169611 - $15.00 USD Received 30 May 2012; revised 17 Jul 2012; accepted 17 Jul 2012; published 23 Jul 2012

characteristics and further work will be required to optimize SESAM performance to exploit this behavior.

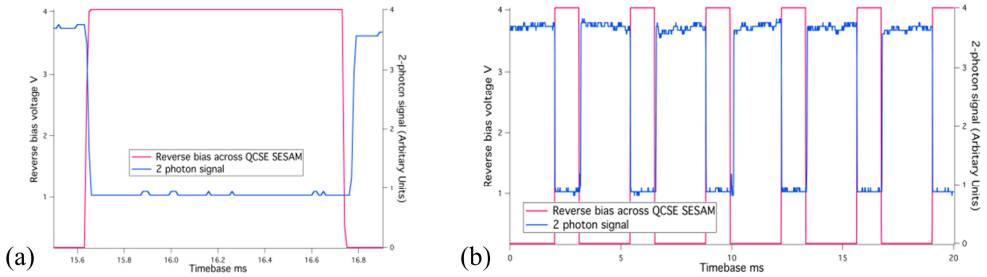

Fig. 4. (a) The reverse-bias signal (red) and 2-photon signal (blue) under switched operation. Note the blue 2-photon trace does not reach zero because picosecond pulses still have sufficient intensity to induce a 2-photon response. (b) Rapid switching between femtosecond and picosecond regimes. In this case, the reverse bias on the QCSE SESAM was modulated at 300 Hz. The output from a two-photon detector is shown in blue and the applied reverse bias in red.

In addition to the regime switching capability of this QCSE SESAM pulse-duration tuning in the picosecond-pulse regime was observed. This was realized in the same laser configuration as described in Fig. 6 when the laser was tuned to a wavelength of 1231 nm via the intracavity slit. Pulse-duration tuning was also observed at longer wavelengths but the range of tuning was severely limited by the onset of unstable femtosecond-pulse operation with increasing reverse bias. The largest degree of duration tuning was observed at a laser output power of 40 mW (with 2.5 W of incident pump light).

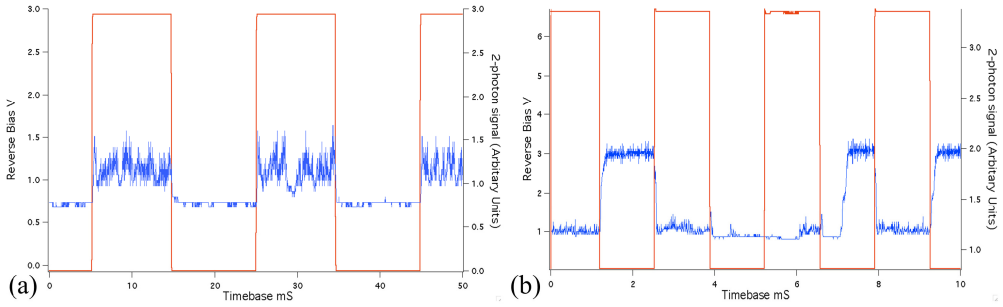

Fig. 5. (a) Observed signal on the two-photon detector blue and corresponding applied reverse bias (red). Note that at this wavelength the laser switches to picosecond operation with an applied bias but with no bias switches to cw operation. (b) Observed signal from the two-photon detector (blue) overlaid with the applied reverse bias (blue). In this case, unstable switching between CW and femtosecond regimes is observed as the reverse bias is changed. In some cases also (e.g. around 6 ms), picosecond operation can also be observed.

The pulse duration was measured to be 6.1 ps with zero bias and decreased monotonically to 1.9 ps at 6 V reverse bias, where the pulse duration plateaued until 8 V reverse bias, at which point pulse duration increased. For these pulse measurements a Gaussian profile provided a closer fit to the autocorrelations and so is assumed here. This increase in pulse duration was accompanied by a drop in laser power, which had remained at a constant 40 mW at lower bias levels. The time-bandwidth product was 0.70 for the shortest pulses (assuming a sech^2 pulse shape) and varied less than 10% through the 0 V to 6 V reverse bias tuning range. The intracavity dispersion compensation was not optimized for operation at this wavelength, nor for picosecond pulses (reducing the dispersive contribution of self phase modulation) and so we believe there is scope to improve this parameter.

#169611 - $15.00 USD Received 30 May 2012; revised 17 Jul 2012; accepted 17 Jul 2012; published 23 Jul 2012

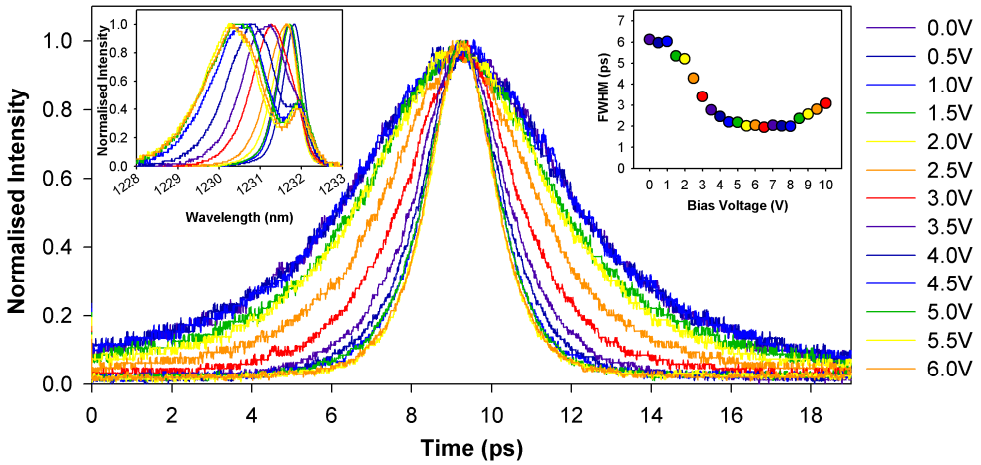

Fig. 6. Main plot: temporal profiles of picosecond pulses measured by intensity autocorrelation under reverse bias levels from 0 V to 6 V. Top left: spectra of pulses corresponding to those in the main plot. Top right: plot showing the evolution of the pulse duration with reverse bias levels up to 10 V.

As the intracavity dispersion was optimized for femtosecond-pulse operation at 1260nm it is proposed that at 1231 nm the soliton mode-locking model no longer applies and pulsing is instead controlled by a form of the fast saturable absorber mechanism. In this regime the pulse duration depends upon the modulation depth of the absorber [16], which is being tuned via the QCSE on application of a reverse bias, thereby explaining the observation of pulse- duration tuning. For the femtosecond pulses obtained in these assessments, it is proposed that the absorber is operating in the soliton regime where pulse formation is affected by a wider range of factors [17] that includes crucially the dispersion present within the system. The degree to which pulse durations can be controlled through electronic adjustment of the SESAM whilst operating in this regime is the subject of ongoing study but our work has shown clearly that the SESAM can be switched successfully between a picosecond operation in the fast saturable absorber regime and a femtosecond operation in the soliton regime.

4. Conclusion

We have demonstrated switching between continuous wave, picosecond and femtosecond operating regimes for a Cr^{4+}:forsterite laser, by exploiting the quantum-confined Stark effect in an electrically contacted GaInNAs SESAM. Additionally, we have demonstrated a continuous tunability of mode-locked pulses in the picosecond regime by a factor of 3.2. Further investigations will include testing the switching capabilities of QCSE SESAMs with alternative absorber designs that enhance the Stark effect and we will investigate more comprehensively the range of pulse durations that can be switched. Using these techniques we believe that it will be possible to develop lasers that exhibit rapid and reliable regime switching with a welcome reduction in their overall complexity.

Acknowledgments

The authors acknowledge the assistance of Dr David Massoubre for his help in wire-bonding the QCSE SESAM and funding from the Engineering and Physical Sciences Research Council (Grants: EP/E064450/1 and EP/E06440X/1.)